ACS OMEGA

http://pubs.acs.org/journal/acsodf

Article

Synthesis and Cytotoxic Activity of Novel Metal Complexes Derived from Methyl-3-(4-chlorophenyl)-3-hydroxy-2,2-dimethylpropanoate as Potential CDK8 Kinase Inhibitors

Ahmed Aboelmagd, Samir M. El Rayes,* Mohamed S. Gomaa, Walid Fathalla, Ibrahim A. I. Ali, Mohamed S. Nafie, Faheem H. Pottoo, Firdos Alam Khan, and Mohamed M. Ibrahim

Cite This: *ACS Omega* 2021, 6, 5244−5254

Read Online

ACCESS | Metrics & More | Article Recommendations | Supporting Information

ABSTRACT: Several metal complexes of methyl-3-(4-chlorophenyl)-3-hydroxy-2,2-dimethylpropanoate derivatives were synthesized and tested for their anti-tumor activities. The ligands include 3-(4-chlorophenyl)-3-hydroxy-2,2-dimethylpropanoic acid (**1**), 3-(4-chlorophenyl)-3-hydroxy-2,2-dimethylpropanehydrazide (**2**), and 3-(4-chlorophenyl)-*N*′-(4-(dimethylamino)benzylidene)-3-hydroxy-2,2-dimethylpropanehydrazide (**3**). The ligands were reacted with Cu (II), Ni (II), and La (III) ions. The formed complexes were characterized using elemental analysis (M%), molar conductivity in DMF (0.001 M), DTA, TG, FTIR, ICP-AES, and magnetic susceptibility. The chemical structures of the obtained complexes were interpreted, and their chemical formulas were postulated. The anti-cancer activities of these complexes were examined on human colorectal carcinoma cells (HCT-116) and also on normal cells (HEK-293). The 48 h post treatments showed that out of 12 compounds, 10 compounds showed inhibitory actions on HCT-116 cells, whereas two compounds did not show any inhibitory actions. Compounds **6c** and **4a** showed the highest inhibitory actions with IC_{50} = 0.154 and 0.18 mM and additionally compounds **3**, **4b**, and **6a** with IC_{50} = 0.267, 0.205, and 0.284 mM, respectively. All tested compounds did not show any inhibitory action on normal HEK-293 cells. Molecular docking results provided a good evidence for activity of the lead compounds **3** and **4a** as CDK8-CYCC kinase inhibitors, which may proposed the mechanism of action toward colon cancer therapy.

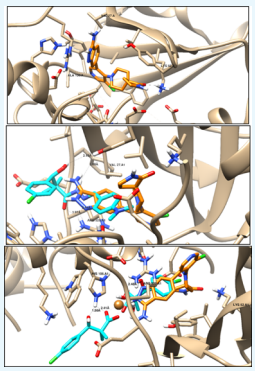

1. INTRODUCTION

There is considerable intrigue within the pharmacology of heterocyclic ligands and their metal chelates. In common, sulfur and nitrogen containing organic compounds and their metal complexes show a wide range of biological activity, as antitumor, antibacterial, antifungal, and antiviral specialists. Copper complexes are broadly utilized in a metal-mediated DNA cleavage for the cycle of enacted oxygen species. It has been detailed that tetra-aza large-scale cyclic copper complexes have showed anti-HIV activities, besides copper amasses in tumors because of the particular penetrability of neoplastic cell membranes to copper compounds. As a result, a number of copper complexes were screened for anticancer activity and few of them were found active both *in vivo* and *in vitro*.[1] One of the successful and effective approaches in the search for new antitumor agents is the development of new metal and rare-earth metal-based anti-cancer agents.[2] Moreover, recent studies show that rare-earth metals and their complexes are superior to transition metals. Rare-earth metals not only have better physiological activities but also have decreased their toxicities after coordinating with a ligand.[3,4] Many Ni(II) complexes showed activity to different tumor cell lines (A549—lung adenocarcinoma cells, MDA-MB-361—breast cancer cell line, HeLa—human cervix carcinoma cells, FemX—melanoma cell line, LS-174—colon cancer cells, K562—human myelogenous leukemia cells, HeLa, FemX, A549, LS-174, MDA-MB-453, and K562) and were more active than the original ligands. Some Ni complexes showed activity to K562 leukemia cells of a similar intensity as cisplatin and were less cytotoxic to the normal MRC-5 cell line (human fetal lung fibroblast cells) than cis platin. Also, many Ni (II) complexes exhibited higher cytotoxicity to K562 cells than to other cell lines. Complexes of Ni(II) interfered with the cell cycle of tumor cells and induced a plasmid DNA cleavage.[5] Moreover, a number of lanthanide complexes have been synthesized and their cytotoxicities were tested and many of lanthanide complexes are expected to be active in preventing tumor growth.[6−8] On the other hand, developments in the fields of inorganic and bioinorganic chemistry have increased the interest in Schiff base complex methods of preparation since it has been recognized that many of these complexes may serve as models for mimicking biomolecules.[9]

Received: October 28, 2020
Accepted: February 5, 2021
Published: February 15, 2021

https://dx.doi.org/10.1021/acsomega.0c05263
ACS Omega 2021, 6, 5244−5254

Scheme 1. Structure of the Target Ligands

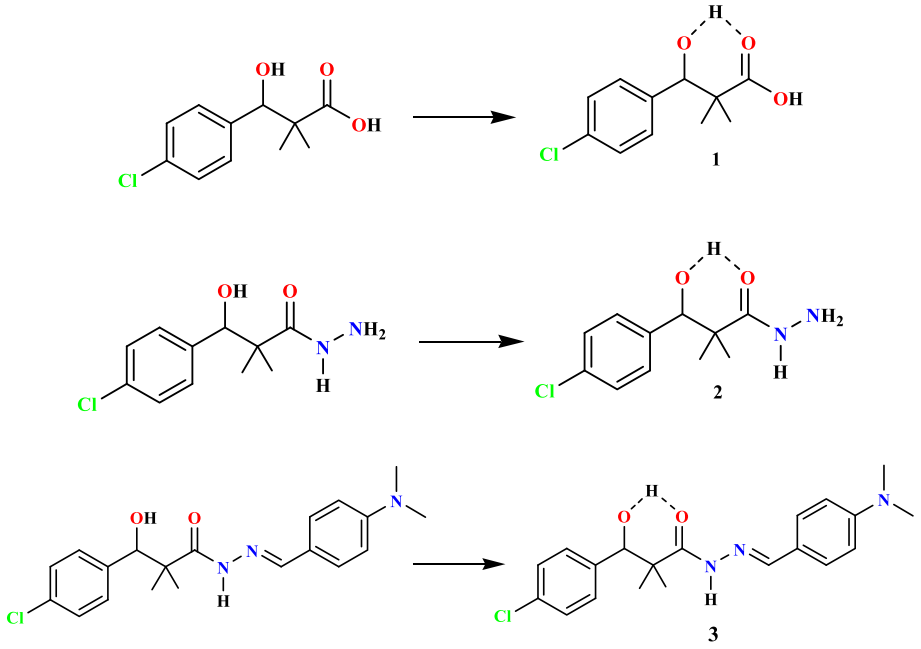

Scheme 2. Postulated Structure of the Synthesized Complexes Derived from Ligand 1

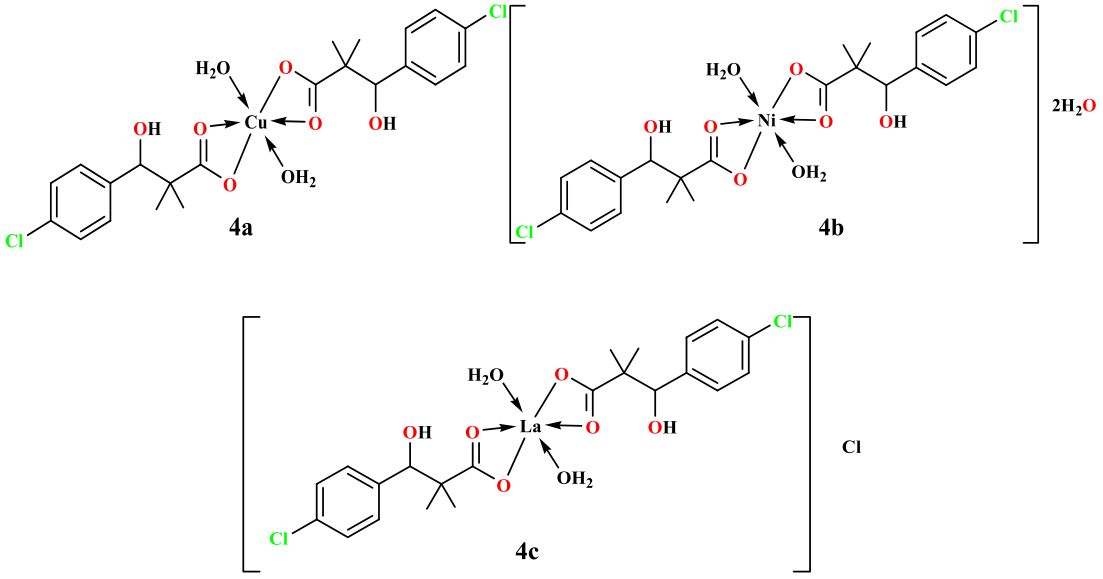

From another perspective, the Schiff's base can also be utilized in cytotoxic drug targeting. The acidic conditions in tumor tissues, endosomes, and lysosomes can be responsible for the cleavage of acid-sensitive prodrugs.[10] Typical examples of acid-sensitive bonds are imine, hydrazone, carboxylic hydrazone, ketal, and acetal. There are many studies suggesting that synthetically designed compounds and complexes showed many biological applications especially as anti-cancer,[11−14] anti-microbial,[15] and anti-inflammatory.[16] Previously, we have reported that treatments of quinoxaline-peptidomimetic derivatives had profound anticancer activity.[17] We have also reported a series of methyl-3-(4-chlorophenyl)-3-hydroxy-2,2-dimethylpropanoate derivatives and their *in vitro* activity on colon cell cancer.[18] The most significant class of human enzymes controlling the sequence of events, including cell cycle progression, cell division, and cell proliferation, is protein kinases.[19] Production of new heterocyclic ligands as an anti-cancer agent is a promising field, and researchers are actively exploring this region to generate new drug candidates.[20] CDK activity is regulated by the combination of CDK inhibitors of regulation and protein (cyclines), phosphorylation, and ubicitin-mediated proteolysis. Since the loss of CDKs that leads to deregulated cell proliferation is one of the hallmarks of cancer, an efficient tumor growth strategy would be anticipated to be implemented in the CDK inhibition and thus impact cancer therapy.[21] Many researchers studied CDK inhibition and employed a number of structural models with varying levels of activities and selectivities.

In continuation to our effort in finding a promising lead for anti-cancer activity, we herein describe the synthesis and testing of novel methyl-3-(4-chlorophenyl)-3-hydroxy-2,2-

https://dx.doi.org/10.1021/acsomega.0c05263
ACS Omega 2021, 6, 5244−5254

Scheme 3. Postulated Structure of the Synthesized Complexes Derived from Ligand 2

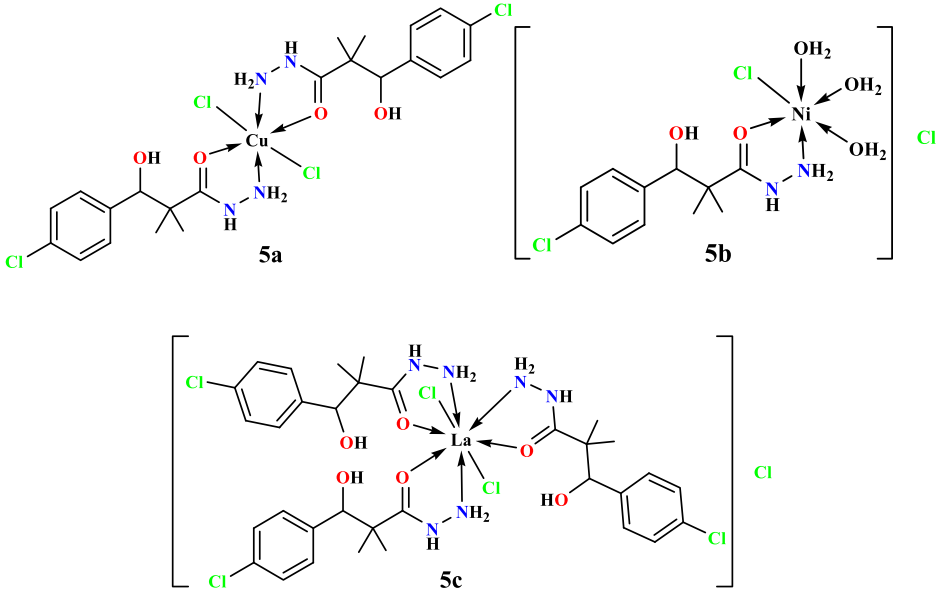

Scheme 4. Postulated Structure of the Synthesized Complexes Derived from Ligand 3

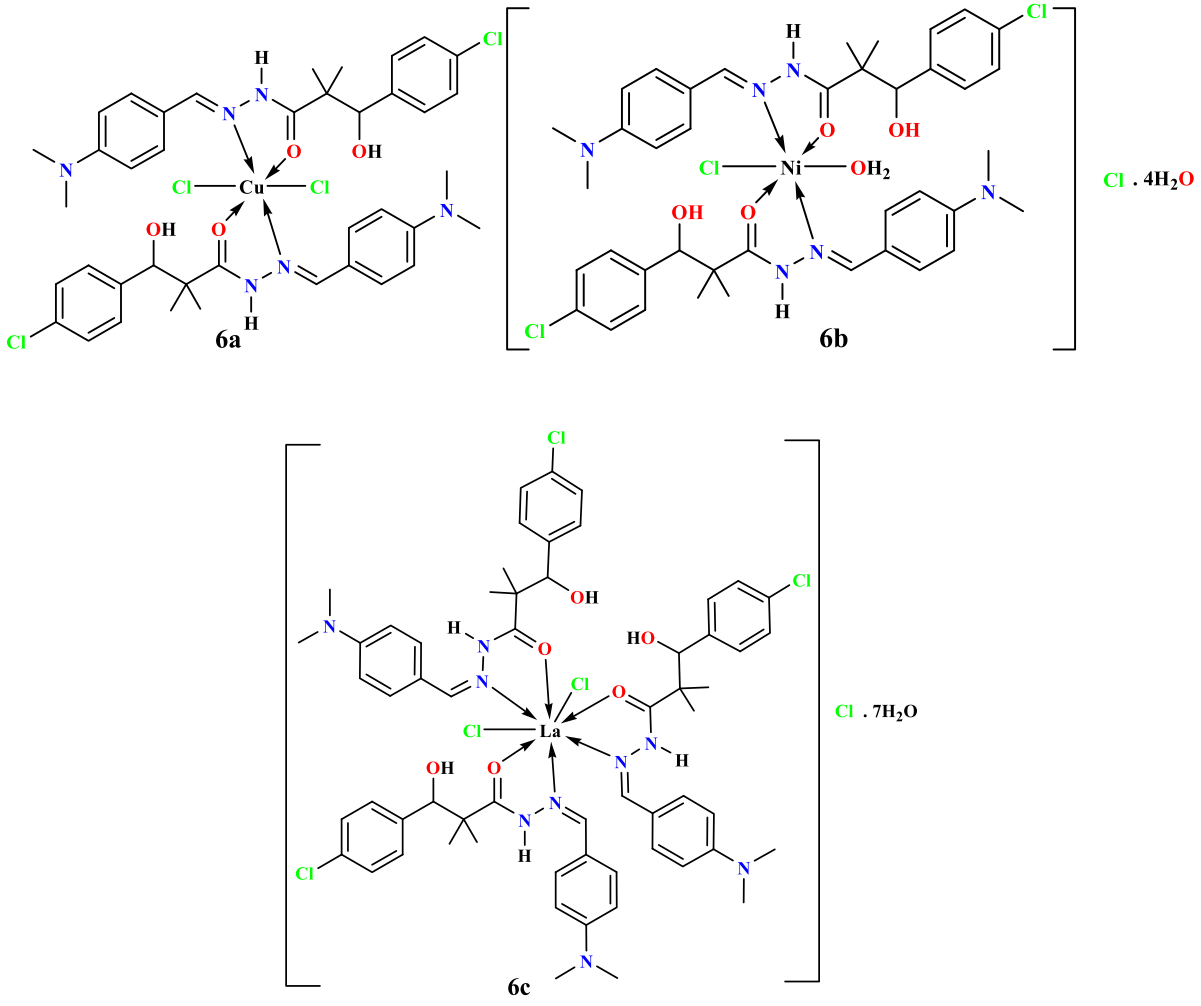

dimethylpropanoate complexes, their action on colon cancer cells and normal cells, and molecular docking study to investigate their activities as cyclin-dependent kinases inhibitors.

https://dx.doi.org/10.1021/acsomega.0c05263
ACS Omega 2021, 6, 5244−5254

2. RESULTS AND DISCUSSION

2.1. Physicochemical Properties of the Target Complexes. The obtained complexes have stable structure and nonhygroscopic behavior at room temperature (Schemes 1−4). The complexes are mostly insoluble in common organic solvents but soluble in DMSO and DMF. Nearly, all complexes are stable and decomposed at temperature greater than 280 °C. The molar conductance values appeared in the range 35−61 μS of 0.001 M DMF solutions at room temperature, which reflect the misleading nature of the formed complexes, which could be considered as non-electrolytic behavior (for the small value) or electrolytic behavior as A+B-salt (for the large conductivity value).[22−24] The elemental analysis, which forced by the thermal analysis, revealed the stoichiometric behavior of the obtained complexes that could be formulated as follows: $[Cu(L^1)_2(H_2O)_2]$(**4a**), $[Ni(L^1)_2(H_2O)_2]\cdot 2H_2O$(**4b**), $[La(L^1)_2(H_2O)_2]Cl$(**4c**), $[Cu(L^2)_2Cl_2]$(**5a**), $[Ni(L^2)(H_2O)_3Cl]Cl$(**5b**), $[La(L^2)_3Cl_2]Cl$(**5c**), $[Cu(L^3)_2Cl_2]$(**6a**), $[Ni(L^3)_2(H_2O)Cl]Cl\cdot 4H_2O$(**6b**), and $[La(L^3)_3Cl_2]Cl\cdot 7H_2O$(**6c**). The obtained data was listed in Tables 1−23.

Table 1. Analytical and Physicochemical Data of the Ligand 1 and its Complexes

Ligand structure		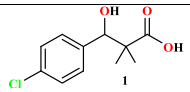		
Complex name		4a	4b	4c
Complex formula		$[Cu(L^1)_2(H_2O)_2]$	$[Ni(L^1)_2(H_2O)_2].2H_2O$	$[La(L^1)_2(H_2O)_2]Cl$
Chemical formula		$C_{22}H_{28}Cl_2CuO_8$	$C_{22}H_{32}Cl_2NiO_{10}$	$C_{22}H_{28}Cl_3LaO_8$
Molecular weight		554.90	586.08	665.71
Color		Green	green	gray
Melting point (°C)		> 280	> 280	>280
M%	calculate	11.45	10.01	20.87
	found	10.90	10.20	21.38
Conductivity		35	41	45
μ_{eff}		2.25	4.04	
Yield %		73	78	64

2.2. FTIR Spectra. The most important IR peaks for the synthesized ligands and their complexes are listed in Table 4. To study the binding mode in the formed complexes, the IR spectra of the ligands were compared with the spectra of their complexes. The acid ligand **1** gave a strong peak centered at 3550 cm^{-1} as a broad peak that could be due to the stretching vibration of the O−H of the carboxylic group and the free OH, which undergoes a hydrogen bond interaction with the neighboring C═O. In case of complex formation, this band showed a small shift due to the replacement of the hydrogen bond by the metal ion, which nearly gave the same bond energy. The weak peaks appeared in the complexes could be due to the M−O and M−N stretching vibrations. All the formed complexes exhibit strong broad bands in the range 3626−3100 cm^{-1} due to the coordinated water molecules.[25]

The hydrazide ligand **2** gave the characteristic peaks, which belong the function groups O−H, C═O, NH, and NH_2 and are shown in Table 4. All complexes gave broad bands with different intensities ranged from 3600 to 3000 cm^{-1} that could

Table 2. Analytical and Physicochemical Data of the Ligand 2 and its Complexes

Ligand structure		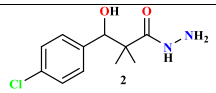		
Complex name		5a	5b	5c
Complex formula		$[Cu(L^2)_2Cl_2]$	$[Ni(L^2)(H_2O)_3Cl]Cl$	$[La(L^2)_3Cl_2]Cl$
Chemical formula		$C_{22}H_{30}Cl_4CuN_4O_4$	$C_{11}H_{21}Cl_3N_2NiO_5$	$C_{33}H_{45}Cl_6LaN_6O_6$
Molecular weight		619.85	426.34	973.36
Color		Blue	blue	yellow
Melting point (°C)		> 280	> 280	>280
M%	calculate	10.25	13.77	14.27
	found	10.10	13.90	13.92
Conductivity		36	61	55
μ_{eff}		1.90	2.98	
Yield %		79	71	66

Table 3. Analytical and Physicochemical Data of the Ligand 3 and its Complexes

Ligand structure		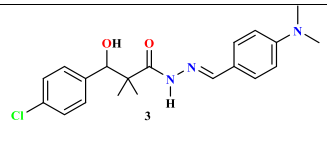		
Complex name		6a	6b	6c
Complex formula		$[Cu(L^3)_2Cl_2]$	$[Ni(L^3)_2(H_2O)Cl]Cl.4H_2O$	$[La(L^3)_3Cl_2]Cl.7H_2O$
Chemical formula		$C_{40}H_{48}Cl_4CuN_6O_4$	$C_{40}H_{58}Cl_4N_6NiO_9$	$C_{60}H_{86}Cl_6LaN_9O_{13}$
Molecular weight		882.21	967.43	1493.00
Color		Brown	Light brown	Shiny yellow
Melting point (°C)		Oil	> 280	> 280
M%	calculate	7.20	6.07	9,30
	found	7.34	6.01	9.80
Conductivity		35	54	55
μ_{eff}			3.11	
Yield %		62	75	76

be due to the presence of H_2O and/or the O−H accompanied by an inter- and/or intrahydrogen bond. C═O and NH_2 gave a noticeable shift on complexation, which indicate the entrance of these groups in the chelation process. M−O and M−N appeared as new peaks, which indicate the complex formation.[26−28]

The hydrazone **3** and its complexes gave the vibration motions of their function groups at the predictable wave number and are listed in Table 4. The stretching vibration wave numbers 3361, 3277, 1649, and 1604 could be from ν_{O-H}, ν_{N-H}, $\nu_{C=O}$, and $\nu_{C=N}$, respectively. The broad band, which ranged from 3600 to 000 cm^{-1}, could be due to the presence of the H_2O molecule in the formed complex as shown in the Ni complex or presence of strong hydrogen-bonded free O−H as shown in complexes Cu and La.[29−31]

2.3. Thermal Analysis. The thermal analysis TGA and DTA gave the best evidence about the presence of water molecules in complexes accompanied with its nature

https://dx.doi.org/10.1021/acsomega.0c05263
ACS Omega 2021, 6, 5244−5254

Table 4. Vibration Wave Number (cm^{-1}) of the Target Ligands and their Complexes[a]

comp.	ν(O−H), (H_2O)	ν(N−H)	$\nu(NH_2)$	ν(C=O)	$\nu(COO)_{assy}$	$\nu(COO)_{sym}$	ν(C=N)	ν(M−O)	ν(M−N)
1	3502 s, br				1682 s	1595 sh			
4a	3498 br				1681 s	1595 sh		446 w	
4b	3626−3100 br				1680 s	1590 sh		446 w	
4c	3626−3100 br				1679 s	1570 sh		480 w	
2	3356 s, br	3265 m	3312 w	1653 s					
5a	3400−3000 br	3241 m	3115 w	1644 s				522 w	450 vw
5b	3300−3100 br	3281 m	3177 w	1647 s				514 w	445 vw
5c	3400−3000 br	3265 m	3312 w	1640 s				525 w	
3	3361 s, br	3227 m		1649 s			1604 m		
6a	3700−3100 br			1601 s			1588 m	508 w	480 vw
6b	3500−3100 br			1649 s			1604 m	530 w	475 vw
6c	3600−3050 br			1649 s			1604 m	530 w	477 vw

[a]s = strong, br = broad, m = medium, w = weak, vw = very weak.

Table 5. Antiproliferative Activity of Synthetic Compounds[a]

Code	Structure of compounds	IC_{50}*#[mM]	
		HCT-116	HEK-293
1	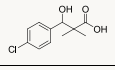	1.27± 0.04	NA
2	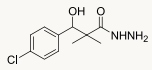	1.65± 0.06	NA
3	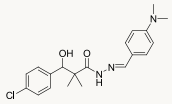	0.267± 0.03	NA
4a	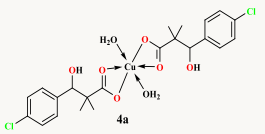	0.18± 0.02	NA
4b	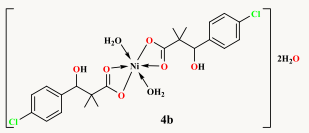	0.205± 0.03	NA
4c	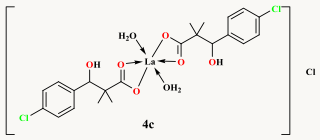	0.933± 0.03	NA
5a	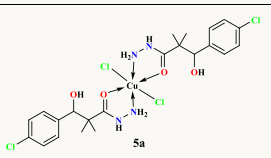	1.037± 0.02	NA
5b	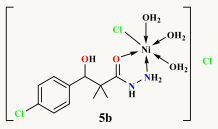	0.353± 0.01	NA
5c	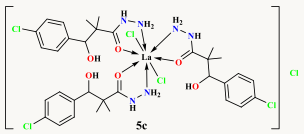	NA	NA
6a	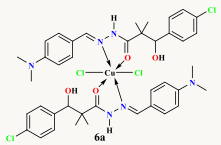	0.284± 0.01	NA
6b	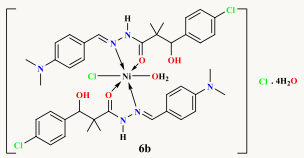	NA	NA
6c	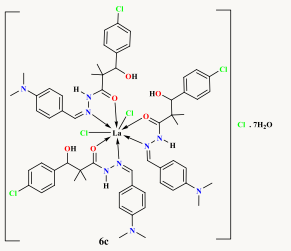	0.154± 0.01	NA

[a]*IC_{50} values (mM) are expressed as mean ± SD of **3** independent trials (n = 3). **NA** is not active (IC_{50} is either not determined or more than 50). #IC_{50} were calculated using GraphPad prism 7 software using a nonlinear regression dose-inhibition curve fit.

(coordinate water or water of crystallization). Complexes **4a** and **4c** have two coordinated water for each, which liberated over 190 °C; meanwhile, **4b** gave two types of water as two coordinated water and 2 as water of crystallization, which liberate in the range centered at 100 °C. Complex **5b** gave thermal behavior accompanied by weight loss revealed the liberation of 3 water molecules in temperature range 200 °C, which indicate the coordinate nature of these molecules. Complex **6b** gave one coordinate water and 4 as water of crystallization, which deduced from percentage of the weight loss and the decomposition temperature. Complex **6c** gave 7 water molecules as water of crystallization.[30−32]

https://dx.doi.org/10.1021/acsomega.0c05263
ACS Omega 2021, 6, 5244−5254

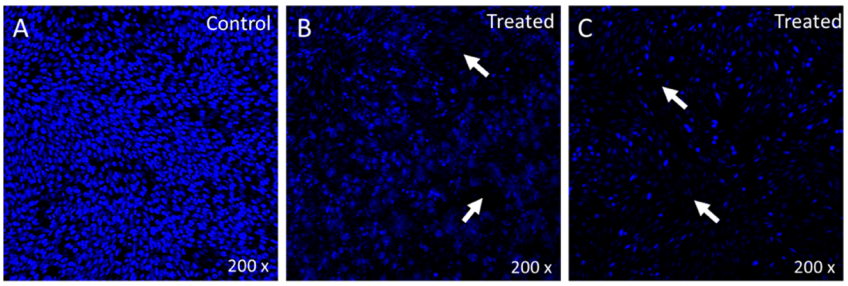

Figure 1. DAPI stained HCT-116 cells. (**A**) Control (nontreated), (**B**) treated with compound **3** (0.1 mg/mL), and (**C**) treated with **4a** compound (0.1 mg/mL). DAPI stained cells visualized through confocal microscope, and Panels (B) and (C) show the significant loss (arrows) of staining due to treatment. 200× magnifications.

2.4. Magnetic Susceptibility. The obtained magnetic moment for **4a** was 2.25 indicating the formation of the OH structure for the Cu (II) complex. The magnetic moment for **4b** was 4.04, which indicates the formation of the high-spin octahedral Ni (II) complex. **5a** and **5b** gave μ_{eff} = 1.9 and 2.98 BM, respectively, due to the formation of octahedral structures for Cu (II) and Ni (II), respectively. The magnetic moment for **6b** was 3.11, which indicates the formation of the distorted octahedral structure for the Ni (II) complex.[33−41]

2.5. Antiproliferative Activities. The capacity of a metal to change the action of a remedially dynamic ligand has been illustrated by illustrations counting a few important to anticancer medications. One reasonable range for the improvement of such prodrugs is transition-metal chemistry where a metal can be utilized to convey and control the movement of a cytotoxic ligand or contribute to the cytotoxicity itself. The point is to invent compounds with a "double trigger" activity, where there is an extra enactment step given by the metal; some time recently, the dynamic species is shaped inside the hypoxic tumor cellular environment. This methodology points to create transition-metal-based prodrugs with progressed natural properties and give a strategy of moving forward upon compounds, which as of now appear a degree of hypoxia selectivity. This when combined with distinction in pH may be utilized to help the enactment of hypoxia-selective prodrugs in conjunction with other properties such as reduction potentials. The utilization of more than one environmental factor to activate such prodrugs could result in improved hypoxia selectivity.

The cytotoxic affect of prepared 12 compounds on cancer cell's practicality was surveyed by MTT measurement. The 48 post treatments appeared that, out of 12 compounds, 10 compounds (**1**, **2**, **3**, **4a**, **4b**, **4c**, **5a**, **5b**, **6a**, and **6c**) showed inhibitory activities on HCT-116 cells, although 2 compounds (**5c** and **6b**) did not appear any inhibitory activities. The inhibitory activities (IC_{50}) of these compounds on both HCT-116 and HEK-293 cells were calculated and found that the compounds **6c** and **4a** appeared to have the most noteworthy inhibitory activities with IC_{50} = 0.154 and 0.18 mM and additionally compounds **3**, **4b**, and **6a** with IC_{50} = 0.267, 0.205, and 0.284 mM, respectively. The IC_{50} values for all 12 compounds are given in Table 5.

The initial ligand **1** appeared with an IC_{50} of 1.27compared to 0.18 and 0.20 mM for its Cu and Ni complexes, respectively. The La complex (**4c**) appeared in a lower action of 0.933 mM, whereas the La complex (**6c**) displayed a powerful movement of 0.154 mM. This was moreover reliable with the Ni complex **5b** of the ligand **2** that had 3 water atoms of crystallization and appeared with an IC_{50} of 0.353 mM compared to 1.65 mM for the first ligand. The IC_{50} values of Cu, Ni, and La complexes were found to be within the range 0.154−0.353 mM. The complexes shown great selectivity as self-evident from their dormancy on ordinary cells. Those complexes speak to great candidates for assisting in investigating and testing to prove their potential predominant action and selectivity compared to their unique cytotoxic ligands. This may be somewhat due to the affectability of the schiff's base complex within the marginally acidic environment in cancer cells, which leads to the hydrolysis of the complex and the discharge of the cytotoxic ligand.

The prevalent action noted for the hydrated complexes may be attributed to the superior penetration and receptor binding due to the nonattendance of a desolvation punishment since the compounds are as of now hydrated and ought to not experience a solvation handle earlier to their tissue infiltration or receptor binding.

The inhibitory activity on typical and noncancerous cells (HEK-293 cells) was inspected to affirm whether these compounds deliver any impacts on them. All compounds were tried on ordinary healthy HEK-293 and MTT cells; the result about uncovered was that all these compounds did not deliver any inhibitory activity on the typical cells, which proposes that synthetized compounds are extraordinarily focusing on cancerous cells. The specificity appeared for those complexes may propose that those compounds might be utilized at higher measurements compared to their original ligand partners to donate superior cytotoxic movement with a less-poisonous quality.

2.6. Nuclear DNA Disintegration. The nuclear disintegration of treated cancerous cells by confocal microscopy was observed. The morphology of untreated (control group) cells remained normal and healthy during the testing phase (Figure 1A).

The treatment of compounds **3** and **4a** showed significant changes in the structure of the cell membrane and cell nucleus. The clear indication of nuclear disintegration, nuclear condensation, and cell death were observed. It was found that **3** and **4a**-treated cells showed the significant loss of nuclear staining (Figure 1B,C) compared to nontreated control (Figure 1A). This loss of staining is due to the loss of the cell nucleus after the treatment of compounds **3** and **4a**, respectively. The nuclear disintegration of cancerous cells is due to programmed cell death, and similar results were also observed in other studies.[42]

2.7. Molecular Docking. In the treatment of cancer, kinase inhibitors are very effective, specifically targeted at particular mutations, primarily responsible for tumorigenesis.

https://dx.doi.org/10.1021/acsomega.0c05263
ACS Omega 2021, 6, 5244−5254

Table 6. Summarized Analysis of Ligand−Receptor Interactions of the Co-Crystallized Ligand and the Lead Compounds 3 and 4a inside the 5FGK Protein[a]

docked compounds	binding affinity (Kcal/mol)	type of interaction	bond length (°A)	interaction moiety involved	amino acid
co-crystallized ligand	−17.32	H-donor	1.92	N−H	C═OVal 27
		H-acceptor	1.7	C═O	N−HLys 52
		H-acceptor	1.95	−N−	N−HAla 100
		arene−cation interaction between the indazole ring and positively charged Arg325 amino acid			
Compound 3	−22.48	H-donor	2.18	C−OH	C═OVal 27
		H-donor	1.80	N−H	C═OVal 27
		H-acceptor	1.97	C═O	N−HArg 325
		H-acceptor	2.44	−N−	N−HArg 325
		arene−arene interactions between two aromatic moieties of *p*-chloro phenyl and His 106 amino acids			
Compound 4a	−20.73	H-acceptor	2.48	C═O[a]	N−HArg 325
		H-acceptor	2.41	C═O[a]	N−HHis 106
		H-acceptor	1.56	C−OH	N−HHis 106
		arene−cation interaction between the *p*-chloro phenyl and positively charged Lys 52 amino acid			

[a]*Carbonyl group coordinated with Cu with the compound structure.

It is divided into substrates that typically have serine, threonine, or tyrosine residues by their capacity to catalyze ATP terminal phosphate transfer.

Cycline-dependent kinases (CDKs) are a family of essential regulatory proteins that regulate various cell functions and are primarily involved in the transcription and cell cycle in many diseases, especially cancer. Therefore, the molecular docking study was performed to investigate the binding interactions toward the CDK8-CYCC kinase inhibitor, which are extremely efficient in the therapy of cancer to elucidate the proposed mechanism of action. 5FGK protein, whose crystal structures complexed with their co-crystallized ligands, was easily accessible from the Protein Data Bank. Ligand receptor interactions with binding affinities (Kcal/mol) of the co-crystallized ligand and the two active compounds **3** and **4a** are highlighted in Table 6 and Figure 2; the co-crystallized ligand of the studied protein forms 3 hydrogen bonds with Val 27, Lys 52, and Ala 100 as the key amino acids for interaction; and compounds **3 and 4a** were docked inside the protein active site of the 5FGK. It formed (1−4) hydrogen bonds with a bond length of ≤2.5 °A through the functional groups either as a hydrogen bond acceptor/donor with the key amino acids like their co-crystallized ligands with binding energies of −22.48 and −20.73 Kcal/mol, respectively. Additionally, they formed van der Waals (arene−arene/arene−cation) interactions with the **His 106** and **Lys 52** amino acids. Our molecular docking results of compounds **3** and **4a** showed good binding affinity toward the tested protein as CDK8-CYCC kinase inhibitors and were in accordance with the potent cytotoxicity results of the two compound against HCT-116 cells, and this may be the proposed mode of action for anti-colon cancer activity.

3. CONCLUSIONS

It was disclosed the synthesis and cytotoxic activity of a series of metal complexes, which derived from methyl-3-(4-chlorophenyl)-3-hydroxy-2,2-dimethylpropanoate derivatives. The complexes were tested on human colorectal carcinoma cells (HCT-116) and on normal health cells (HEK-293). The IC_{50} value was found to be in the range 0.154−1.037 mM. The complexes exhibited good selectivity as obvious from their inactivity on normal cells. Those Cu, Ni, and La complexes represent good candidates for further research and testing to proof their potential superior activity and selectivity compared to their original cytotoxic ligands. Molecular docking results provided a good evidence for activity of the lead compounds **3** and **4a** as CDK8-CYCC kinase inhibitors, which may proposed the mechanism of action toward colon cancer therapy. Therefore, from these results, it is recommended to further test the cell cycle analysis for apoptotic investigation, additionally, *in vivo* cancer model for the compounds so that it can be developed as a chemotherapeutic anti-cancer agent.

4. EXPERIMENTAL SECTION

4.1. Materials. All chemicals used in this study were of analytical grade. The chemicals (Koch-Light and Sigma-Aldrich) were used as received. The metal chloride salts (Cu (II), Ni (II), and La (III)) were purchased from the Sigma-Aldrich and used without extra treatment. The working ligands were prepared and characterized according to the previous work.[43]

4.2. Synthesis of the Target Complexes. *4.2.1. Synthesis of Copper Complex **4a** of Methyl-3-(4-chlorophenyl)-3-hydroxy-2,2-dimethylpropanoic Acid **1**.* The acid **1** (0.86 g, 3 mmol) was dissolved in hot aqueous ethanol (15 mL). The acid solution was added to a solution of cupric chloride $CuCl_2{\cdot}2H_2O$ (0.25 g, 1.5 mmol) in ethanol. Under reflux with stirring, the reaction mixture was left for 4 h. The reaction mixture was evaporated to about 20% of the original volume. Then, the pH was adjusted to 7. The formed precipitate was filtered off, washed with cold ethanol and ether, and dried in vacuum at room temperature in a desiccator in the presence of CaO.

*4.2.2. Synthesis of Nickel Complex **4b** of Methyl-3-(4-chlorophenyl)-3-hydroxy-2,2-dimethylpropanoic Acid **1**.* The nickel complex **4b** is obtained by reflexing the ethanolic solution of the acid **1** (0.86 g, 3 mmol) and nickel chloride $NiCl_2{\cdot}6H_2O$ (0.35 g, 1.5 mmol). After 4 h, the reaction was worked up the same as done with the copper complex **4a**.

*4.2.3. Synthesis of Lanthanum Complex **4c** of Methyl-3-(4-chlorophenyl)-3-hydroxy-2,2-dimethylpropanoic Acid **1**.* The lanthanum complex **4c** is prepared by heating a solution of the acid **1** (0.86 g, 3 mmol) and lanthanum chloride $LaCl_3{\cdot}$

https://dx.doi.org/10.1021/acsomega.0c05263
ACS Omega 2021, 6, 5244−5254

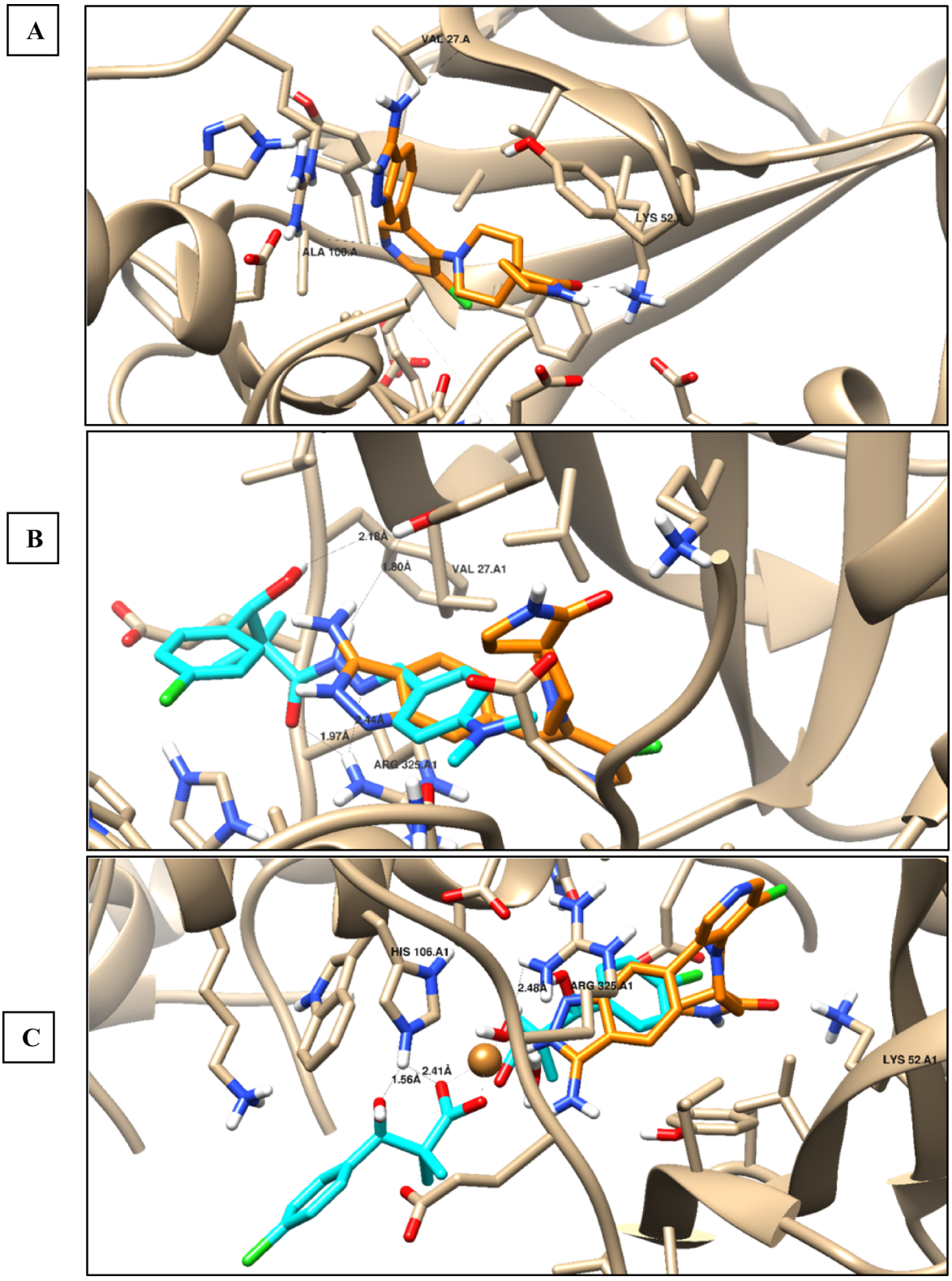

Figure 2. Superimposition and ligand−receptor interactions of (A), theco-crystallized ligand (orange), and (B) and (C) are the lead compounds **3** and **4a** (green), respectively, inside the 5FGK binding site.

$6H_2O$ (0.53 g, 1.5 mmol) in ethanol under reflux for 4 h. The obtained solution was concentrated to about 20% of the original volume; then the pH was adjusted to 5. The formed complex was filtered, washed with cold ethanol and ether, and dried in vacuum at room temperature in a desiccator in the presence of CaO.

*4.2.4. Synthesis of Copper Complex **5a** of Methyl-3-(4-chlorophenyl)-3-hydroxy-2,2-dimethylpropanoyl Hydrazide **2**.* A solution of cupric chloride $CuCl_2{\cdot}2H_2O$ (0.25 g, 1.5 mmol) in ethanol was added to the solution of the hydrazide **2** (0.72 g, 3 mmol) in hot aqueous ethanol (15 mL). The reaction mixture was refluxed under stirring for 4 h. The

https://dx.doi.org/10.1021/acsomega.0c05263
ACS Omega 2021, 6, 5244−5254

reaction was worked up the same as done with the copper complex **4a**.

*4.2.5. Synthesis of Nickel Complex **5b** of Methyl-3-(4-chlorophenyl)-3-hydroxy-2,2-dimethylpropanoyl Hydrazide **2**.* The nickel complex **5b** is obtained by reflexing the ethanolic solution of the hydrazide **2** (0.72 g, 3 mmol) and nickel chloride $NiCl_2{\cdot}6H_2O$ (0.35 g, 1.5 mmol). After 4 h, the reaction was worked up the same as done with the copper complex **4a**.

*4.2.6. Synthesis of Lanthanum Complex **5c** of Methyl-3-(4-chlorophenyl)-3-hydroxy-2,2-dimethylpropanoyl Hydrazide **2**.* The lanthanum complex **5c** is prepared by heating a solution of the hydrazide **2** (0.86 g, 3 mmol) and lanthanum chloride $LaCl_3{\cdot}6H_2O$ (0.53 g, 1.5 mmol) in ethanol under reflux for 4 h. The reaction was worked up the same as done with the copper complex **4c**.

*4.2.7. Synthesis of Copper Complex **6a** of Methyl-3-(4-chlorophenyl)-3-hydroxy-2,2-dimethylpropanoyl Hydrazone Derivative **3**.* To the solution of the hydrazone **3** (1.12 g, 3 mmol) in hot aqueous ethanol (15 mL), a solution of cupric chloride $CuCl_2{\cdot}2H_2O$ (0.25 g, 1.5 mmol) in ethanol was added. The reaction mixture was refluxed under stirring for 4 h. The obtained solution was evaporated to about 20% of the original volume. Then, the pH was adjusted to 7. The complex **6a** is obtained as oil and extracted by diethyl ether.

*4.2.8. Synthesis of Nickel Complex **6b** of Methyl-3-(4-chlorophenyl)-3-hydroxy-2,2-dimethylpropanoyl Hydrazone Derivative **3**.* The nickel complex **6b** is obtained by refluxing the ethanolic solution of the hydrazone **3** (1.12 g, 3 mmol) and nickel chloride $NiCl_2{\cdot}6H_2O$ (0.35 g, 1.5 mmol). After 4 h, the reaction was worked up the same as done with the copper complex **4a**.

*4.2.9. Synthesis of Lanthanum Complex **6c** of Methyl-3-(4-chlorophenyl)-3-hydroxy-2,2-dimethylpropanoyl Hydrazone Derivative **3**.* The lanthanum complex **5c** is prepared by heating a solution of the hydrazone **3** (1.12 g, 3 mmol) and lanthanum chloride $LaCl_3{\cdot}6H_2O$ (0.53 g, 1.5 mmol) in ethanol under reflux for 4 h. The reaction was worked up the same as done with the copper complex **4c**.

4.3. Physical Measurements. The M% (Cu and Ni) content was determined by complexometry using an EDTA titrant and murexide as an indicator at pH = 10 using ammonia buffer, while the La % content was determined using inductively coupled plasma atomic emission spectroscopy (ICP atomic absorption spectroscopy).

The FTIR spectra were recorded using KBr disc in the 4000−400 cm^{-1} wave number range on a Bruker Vector 22 spectrometer. DTG and DTA were recorded on a Shimadzu 60 thermal analyzer under a dynamic flow of nitrogen (20 mL/min) and heating rates = 5 and 10 °C/min, from ambient temperature to 800 °C. Electrical conductivity measurements were carried out at room temperature on freshly prepared 0.001 M solutions using a WTW conductivity meter fitted with a L100 conductivity cell. Magnetic susceptibility measurements were carried out using the modified Gouy method on a MSB-MK1 balance at room temperature using mercury (II) tetrathiocyanatecobaltate (II).

4.4. Antiproliferative Activity by the MTT Assay. The anti-proliferative activity of bothnon-cancerous cells (human embryonic kidney cells: HEK-293) and cancerous cells (human colorectal carcinoma cells: HCT-116) was done by the MTT assay. The cell culture and MTT assay were done as per previously described method.[44] However, we have described the method in brief. Cells were grown in 96-well plates in the culture media containing DMEM, L-glutamine, fetal bovine serum, selenium chloride, and penicillin-streptomycin. The cells were treated with different concentrations (0.06−0.7 mg/mL) of 12 synthetic compounds. In the control group, no synthetic compounds were added. After 48 h of treatments, MTT (5.0 mg/mL) was added in each well and was kept incubated for 4 h. Thereafter, DMSO was added and plates were read at a 570 nm wavelength using an ELISA Plate Reader (Biotek Instruments, Winooski, USA). The percentage (%) of cell viability (%) was calculated, and all statistical analyses were completed with Graph Pad Prism 6 (Graph Pad Software). The difference between control and compound-treated groups by a one-way analysis of variance (ANOVA) and *p*-values were calculated by the Student's *t*-test.

4.5. Nuclear DNA Staining. We examined status of nuclear disintegration of cancerous cells after treatments by staining with DAPI (4′,6-diamidino-2-phenylindole). We have selected compounds **3** and **4a**, which showed the highest inhibitory action on the HCT-116 cell for the DAPI staining. The cancerous (HCT-116) cells were treated with 0.1 mg/mL concentration. In control group, compounds **3** and **4a** were not added. After 48 h of treatment, both control and compounds **3** and **4a**-treated groups were immersed in 4% paraformaldehyde solution. Thereafter, fixed cells were treated with Triton X-100+phosphate buffered saline (PBS). Both control and compounds **3** and **4a**-treated cells were stained with DAPI. The nuclear staining of both control and compound-treated cells was examined under a confocal scanning microscope (Zeiss Germany).

4.6. Molecular Docking. Kinase inhibitors cyclin-dependent kinase 8 (CDK8) are extremely efficient in the therapy of cancer,[45] so the synthesized derivatives were subjected to molecular docking studies toward CDK8-CYCC(PDB = 5FGK, https://www.rcsb.org/structure/5FGK) protein whose structure with the co-crystallized ligand well characterized through XRD with good parameters, resolution lower than 2.5 and with an acceptable *R*-value free 0.237. All molecular modeling studies were performed on a computational software basis using the (MOE 2015-10 Chemical Computing Group, Canada) to evaluate their binding affinities toward this proposed target. Principles of modeling regarding receptor and ligand preparation and molecular docking were carried out according to Nafie et al.[46] Each ligand−receptor complex was tested for binding interaction analysis; 3D images were taken by Chimera as visualizing software.

■ ASSOCIATED CONTENT

Supporting Information

The Supporting Information is available free of charge at https://pubs.acs.org/doi/10.1021/acsomega.0c05263.

A series of metal complexes from methyl-3-(4-chlorophenyl)-3-hydroxy-2,2-dimethylpropanoate derivatives were obtained, Cu and Ni complexes showed higher activity compared to La complexes against human colorectal carcinoma cells(HCT-116) and on normal health cells (HEK-293), the more hydrated crystals were the most active, the IC_{50} was in the range 0.1−0.64 mg/mL, the complexes exhibited good selectivity as obvious from their inactivity on normal cells, and the mechanism of action toward colon cancer

https://dx.doi.org/10.1021/acsomega.0c05263
ACS Omega 2021, 6, 5244−5254

therapy was provided *via* molecular docking studies (PDF)

AUTHOR INFORMATION

Corresponding Author

Samir M. El Rayes − *Department of Chemistry, Faculty of Science, Suez Canal University, Ismailia 41522, Egypt;* orcid.org/0000-0003-2667-3855; Phone: +20127500914; Email: samir_elrayes@yahoo.com

Authors

Ahmed Aboelmagd − *Department of Chemistry, Faculty of Science, Suez Canal University, Ismailia 41522, Egypt*

Mohamed S. Gomaa − *Department of Pharmaceutical, College of Clinical Pharmacy, ImamAbdulrahman Bin Faisal University, Dammam 31441, Kingdom of Saudi Arabia*

Walid Fathalla − *Department of Physics and Math, Faculty of Engineering, Port-Said University, Port-Said 42526, Egypt*

Ibrahim A. I. Ali − *Department of Chemistry, Faculty of Science, Suez Canal University, Ismailia 41522, Egypt*

Mohamed S. Nafie − *Department of Chemistry, Faculty of Science, Suez Canal University, Ismailia 41522, Egypt;* orcid.org/0000-0003-4454-6390

Faheem H. Pottoo − *Department of Pharmacology, College of Clinical Pharmacy, Imam Abdulrahman Bin Faisal University, Dammam 31441, Kingdom of Saudi Arabia*

Firdos Alam Khan − *Department of Stem Cell Research, Institute of Research and Medical consultations (IRMC), Imam Abdulrahman Bin Faisal University, Dammam 31441, Saudi Arabia;* orcid.org/0000-0002-6892-1530

Mohamed M. Ibrahim − *Department of Chemistry, College of Science, Taif University, Taif 21944, Saudi Arabia*

Complete contact information is available at: https://pubs.acs.org/10.1021/acsomega.0c05263

Notes

The authors declare no competing financial interest.

ACKNOWLEDGMENTS

We would like to thank the Science & Technology Development Fund in Egypt STDF Project ID: 22909 and to Taif University Researchers Supporting Project number (TURSP-2020/05), Taif University, Taif, Saudi Arabia for funding this research proposal.

REFERENCES

(1) Arjmand, F.; Mohani, B.; Ahmad, S. Synthesis, antibacterial, antifungal activity and interaction of CT-DNA with a new benzimidazole derived Cu(II) complex. *Eur. J. Med. Chem.* **2005**, *40*, 1103−1110.

(2) Andiappan, K.; Sanmugam, A.; Deivanayagam, E.; Karuppasamy, K.; Kim, H.-S.; Vikraman, D. In vitro cytotoxicity activity of novel Schiff base ligand-lanthanide complexes. *Sci. Rep.* **2018**, *8*, 3054.

(3) Saturnino, C.; Napoli, M.; Paolucci, G.; Bortoluzzi, M.; Popolo, A.; Pinto, A.; Longo, P. Synthesis and cytotoxic activities of group 3 metal complexes having monoanionic tridentate ligands. *Eur. J. Med. Chem.* **2010**, *45*, 4169−4174.

(4) Caporale, A.; Palma, G.; Mariconda, A.; del Vecchio, V.; Iacopetta, D.; Parisi, O. I.; Sinicropi, M. S.; Puoci, F.; Arra, C.; Longo, P.; Saturnino, C. Synthesis and Antitumor Activity of New Group 3 Metallocene Complexes. *Molecules* **2017**, *22*, 526.

(5) Čobeljić, B.; Milenković, M.; Pevec, A.; Turel, I.; Vujčić, M.; Janović, B.; Gligorijević, N.; Sladić, D.; Radulović, S.; Jovanović, K.; Anđelković, K. Investigation of antitumor potential of Ni(II) complexes with tridentate PNO acylhydrazones of 2-(diphenylphosphino)benzaldehyde and monodentate pseudohalides. *J. Biol. Inorg. Chem.* **2016**, *21*, 145−162.

(6) Azab, H. A.; Hussein, B. H. M.; El-Azab, M. F.; Gomaa, M.; El-Falouji, A. I. Bis(acridine-9-carboxylate)-nitro-europium(III) dihydrate complex a new apoptotic agent through Flk-1 down regulation, caspase-3 activation and oligonucleosomes DNA fragmentation. *Bioorg. Med. Chem.* **2013**, *21*, 223−234.

(7) Hussein, B. H. M.; Azab, H. A.; El-Azab, M. F.; El-Falouji, A. I. A novel anti-tumor agent, Ln(III) 2-thioacetate benzothiazole induces anti-angiogenic effect and cell death in cancer cell lines. *Eur. J. Med. Chem.* **2012**, *51*, 99−109.

(8) Chen, Z.-F.; Tan, M.-X.; Liu, Y.-C.; Peng, Y.; Wang, H.-H.; Liu, H. G.; Liang, H. Synthesis, characterization and preliminary cytotoxicity evaluation of five Lanthanide(III)−Plumbagin complexes. *J. Inorg. Biochem.* **2011**, *105*, 426−434.

(9) Khan, S. A.; Nami, S. A. A.; Bhat, S. A.; Kareem, A.; Nishat, N. Synthesis, characterization and antimicrobial study of polymeric transition metal complexes of Mn(II), Co(II), Ni(II), Cu(II) and Zn(II). *Microb. Pathog.* **2017**, *110*, 414−425.

(10) Tannock, I. F.; Rotin, D. Acid pH in Tumors and Its Potential for Therapeutic Exploitation. *Cancer Res.* **1989**, *49*, 4373−4384.

(11) Hajri, M.; Esteve, M.-A.; Khoumeri, O.; Abderrahim, R.; Terme, T.; Montana, M.; Vanelle, P. Synthesis and evaluation of in vitro antiproliferative activity of new ethyl 3-(arylethynyl)-quinoxaline-2-carboxylate and pyrido[4,3-b]quinoxalin-1(2H)-one derivatives. *Eur. J. Med. Chem.* **2016**, *124*, 959−966.

(12) Ingle, R.; Marathe, R.; Magar, D.; Patel, H. M.; Surana, S. J. Sulphonamido-quinoxalines: search for anticancer agent. *Eur. J. Med. Chem.* **2013**, *65*, 168−186.

(13) Piras, S.; Loriga, M.; Paglietti, G. Quinoxaline chemistry. Part XVII. Methyl [4-(substituted 2-quinoxalinyloxy) phenyl] acetates and ethyl N-{[4-(substituted 2-quinoxalinyloxy) phenyl] acetyl} glutamates analogs of methotrexate: synthesis and evaluation of in vitro anticancer activity. *Farmaco* **2004**, *59*, 185−194.

(14) Barea, C.; Pabón, A.; Castillo, D.; Zimic, M.; Quiliano, M.; Galiano, S.; Pérez-Silanes, S.; Monge, A.; Deharo, E.; Aldana, I. New salicylamide and sulfonamide derivatives of quinoxaline 1,4-di-N-oxide with antileishmanial and antimalarial activities. *Bioorg. Med. Chem. Lett.* **2011**, *21*, 4498−4502.

(15) Ramalingam, P.; Ganapaty, S.; Rao, C. B. In vitro antitubercular and antimicrobial activities of 1-substituted quinoxaline-2,3(1H,4H)-diones. *Bioorg. Med. Chem. Lett.* **2010**, *20*, 406−408.

(16) Abu-Hashem, A. A.; Gouda, M. A.; Badria, F. A. Synthesis of some new pyrimido [2′,1′:2,3]thiazolo[4,5-b]quinoxaline derivatives as anti-inflammatory and analgesic agents. *Eur. J. Med. Chem.* **2010**, *45*, 1976−1981.

(17) el Rayes, S. M.; Aboelmagd, A.; Gomaa, M. S.; Ali, I. A. I.; Fathalla, W.; Pottoo, F. H.; Khan, F. A. Convenient synthesis and anticancer activity of methyl 2-[3-(3-phenyl-quinoxalin-2-ylsulfanyl)-propanamido]alkanoates and N-Alkyl 3-((3-phenylquinoxalin-2-yl)-sulfanyl)propanamides. *ACS Omega* **2019**, *4*, 18555−18566.

(18) el-Rayes, S.; Gomaa, M. S.; Abouelmagd, A.; Fathalla, W.; Ali, I. A. I. Synthesis and antiproliferative assay of triazolyl-2,2-dimethyl-3-phenylpropanoates as potential HDAC inhibitors. *RSC Adv.* **2019**, *9*, 13896−13907.

(19) Vermeulen, K.; Van Bockstaele, D. R.; Berneman, Z. N. The cell cycle: a review of regulation, deregulation and therapeutic targets in cancer. *Cell Proliferation* **2003**, *36*, 131−149.

(20) Tantawy, E. S.; Amer, A. M.; Mohamed, E. K.; Abd Alla, M. M.; Nafie, M. S. Synthesis, characterization of some pyrazine derivatives as anti-cancer agents: In vitro and in Silico approaches. *J. Mol. Struct.* **2020**, *1210*, 128013.

(21) Ding, L.; Cao, J.; Lin, W.; Chen, H.; Xiong, X.; Ao, H.; Yu, M.; Lin, J.; Cui, Q. The Roles of Cyclin-Dependent Kinases in Cell-Cycle

Progression and Therapeutic Strategies in Human Breast Cancer. *Int. J. Mol. Sci.* **2020**, *21*, 1960.
(22) Orabi, A. Mercury Complexes Derived From Some Acetone Derivatives Ligands. *Afinidad* **2012**, *69*, 53−61.
(23) Orabi, A. S.; Deghaidy, F. S.; Azab, H. A.; Said, H. Physico-Chemical Properties of Nd(III) and Er(III) Complexes With Some Biological Buffer Ligands. *Synth. React. Inorg. Met.-Org. Chem.* **2001**, *31*, 695−711.
(24) Orabi, A. S.; Abou El-Nour, K. M.; Youssef, M. F.; Salem, H. A. Novel and highly effective composites of silver and zinc oxide nanoparticles with some transition metal complexes against different microorganisms. *Arabian J. Chem.* **2020**, 2628−2648.
(25) Kitching, M.; Ramani, M.; Marsili, E. Fungal biosynthesis of gold nanoparticles: mechanism and scale up. *Microb. Biotechnol.* **2015**, *8*, 904−917.
(26) Günzler, H.; Williams, A. *Handbook of Analytical Techniques*, 2008, DOI: 10.1002/9783527618323.
(27) Rama, I.; Selvameena, R. Synthesis, structure analysis, anti-bacterial and in vitro anti-cancer activity of new Schiff base and its copper complex derived from sulfamethoxazole. *Chem. Sci.* **2015**, *127*, 671−678.
(28) Thomas, K. D.; Adhikari, A. V.; Telkar, S.; Chowdhury, I. H.; Mahmood, R.; Pal, N. K.; Row, G.; Sumesh, E. Design, synthesis and docking studies of new quinoline-3-carbohydrazide derivatives as antitubercular agents. *Eur. J. Med. Chem.* **2011**, *46*, 5283−5292.
(29) Rodríguez, F. J.; Schlenger, P.; García-Valverde, M. A comprehensive structural evaluation of humic substances using several fluorescence techniques before and after ozonation. Part I: Structural characterization of humic substances. *Sci. Total Environ.* **2014**, *476-477*, 718−730.
(30) Ajibade, P. A.; Idemudia, O. G. Synthesis, Characterization, and Antibacterial Studies of Pd(II) and Pt(II) Complexes of Some Diaminopyrimidine Derivatives. *Bioinorg. Chem. Appl.* **2013**, 549549.
(31) Abdel-Rahman, L. H.; El-Khatib, R. M.; Nassr, L. A. E.; Abu-Dief, A. M.; Ismael, M.; Seleem, A. A. Metal based pharmacologically active agents: Synthesis, structural characterization, molecular modeling, CT-DNA binding studies and in vitro antimicrobial screening of iron(II) bromosalicylidene amino acid chelates. *Spectrochim. Acta, Part A* **2014**, *117*, 366−378.
(32) Soliman, A. A.; Ali, S. A.; Orabi, A. Spectral and thermal studies of some chromium and molybdenum complexes with ONO donor Schiff bases. *Spectrochim. Acta, Part A* **2006**, *65*, 841−845.
(33) Sundararajan, M. L.; Jeyakumar, T.; Anandakumaran, J.; Karpanai Selvan, B. Synthesis of metal complexes involving Schiff base ligand with methylenedioxy moiety: Spectral, thermal, XRD and antimicrobial studies. *Spectrochim. Acta, Part A* **2014**, *131*, 82−93.
(34) Orabi, A. S.; Abbas, A. M.; Sallam, S. A. Spectral, magnetic, thermal, and DNA interaction of Ni(II) complexes of glutamic acid schiff bases. *Synth. React. Inorg., Met.-Org., Nano-Met. Chem.* **2013**, *43*, 63−75.
(35) Chaudhary, N. K.; Mishra, P. Bioactivity of some divalent M(II) complexes of penicillin based Schiff base ligand: Synthesis, spectroscopic characterization, and thermal study. *J. Saudi Chem. Soc.* **2018**, *22*, 601.
(36) Sallam, S. A.; Orabi, A. S.; Abbas, A. M. DNA interaction with octahedral and square planar Ni(II) complexes of aspartic-acid Schiff-bases. *J. Mol. Struct.* **2011**, *1006*, 272−281.
(37) Małecki, J. G.; Bałanda, M.; Groń, T.; Kruszyński, R. Molecular, spectroscopic, and magnetic properties of cobalt(II) complexes with heteroaromatic N(O)-donor ligands. *J. Struct. Chem.* **2012**, *23*, 1219−1232.
(38) Barefield, E. K.; Busch, D. H.; Nelson, S. M. Iron, cobalt, and nickel complexes having anomalous magnetic moments. *Q. Rev., Chem. Soc.* **1968**, *22*, 457−498.
(39) Teweldemedhin, Z. S.; Fuller, R. L.; Greenblatt, M. Magnetic Susceptibility Measurements of Solid Manganese Compounds with Evan's Balance. *J. Chem. Educ.* **1996**, *73*, 906−909.
(40) Orabi, A. S. Physical Properties of Some New Uranyl Complexes with Ligands Derived from Acetone. *Monatsh. Chem.* **1998**, *129*, 1139−1149.
(41) Chandra, S.; Pipil, P. Synthesis, Spectral Characterization and Biological Evaluation of Chromium(III) Complexes of Schiff Base. *Open J. Inorg. Chem.* **2014**, *04*, 30−40.
(42) Khan, F. A.; Akhtar, S.; Almofty, S. A.; Almohazey, D.; Alomari, M. FMSP-Nanoparticles Induced Cell Death on Human Breast Adenocarcinoma Cell Line (MCF-7 Cells): Morphometric Analysis. *Biomolecules* **2018**, *8*, 32−44.
(43) Bahgat, K.; Orabi, A. S. Physical characteristics, vibrational spectroscopy and normal-coordinate analysis of 2-aminophenol and 2-phenylenediamine complexes. *Polyhedron* **2002**, *21*, 987.
(44) Rehman, S.; Asiri, S. M.; Khan, F. A.; Jermy, B. R.; Ravinayagam, V.; Alsalem, Z.; Jindan, R. A.; Qurashi, A. Anticandidal and In vitro Anti-Proliferative Activity of Sonochemically synthesized Indium Tin Oxide Nanoparticles. *Sci. Rep.* **2020**, *10*, 3228.
(45) Bhullar, K. S.; Lagarón, N. O.; McGowan, E. M.; Parmar, I.; Jha, A.; Hubbard, B. P.; Rupasinghe, H. P. V. Kinase-targeted cancer therapies: progress, challenges and future directions. *Mol. Cancer.* **2018**, *17*, 48.
(46) Nafie, M. S.; Tantawy, M. A.; Elmgeed, G. A. Screening of different drug design tools to predict the mode of action of steroidal derivatives as anti-cancer agents. *Steroids* **2019**, *152*, 108485.

https://dx.doi.org/10.1021/acsomega.0c05263
ACS Omega 2021, 6, 5244−5254